Title

Methods for implantation of micro-wire bundles and optimization of single/multi-unit recordings from human mesial temporal lobe

Journal

Journal of Neural Engineering, 11(2)

ISSN

1741-2560

Authors

Misra, A
Burke, JF
Ramayya, AG
et al.

Publication Date

2014-04-01

DOI

10.1088/1741-2560/11/2/026013

Peer reviewed

Published in final edited form as:
J Neural Eng. 2014 April ; 11(2): 026013. doi:10.1088/1741-2560/11/2/026013.

Methods for implantation of micro-wire bundles and optimization of single/multiunit recordings from human mesial temporal lobe

A Misra[1,*], **JF Burke**[2,*], **A Ramayya**[2], **J Jacobs**[1], **MR Sperling**[3], **KA Moxon**[1,6], **MJ Kahana**[4], **JJ Evans**[5], and **AD Sharan, M.D.**[5]

[1]College of Biomedical Engineering Science and Healthcare Systems Drexel University, Philadelphia PA 19104, USA

[2]Neuroscience Graduate Group, University of Pennsylvania, Philadelphia PA, 19104, USA

[3]Dept. of Neurology, Thomas Jefferson University, Philadelphia PA 19107, USA

[4]Dept. of Psychology, University of Pennsylvania, Philadelphia PA, 19104, USA

[5]Dept. of Neurological Surgery, Thomas Jefferson University, Philadelphia PA 19107, USA

Abstract

Objective—The authors report methods developed for the implantation of micro-wire bundles into mesial temporal lobe structures and subsequent single neuron recording in epileptic patients undergoing in-patient diagnostic monitoring. This is done with the intention of lowering the perceived barriers to routine single neuron recording from deep brain structures in the clinical setting.

Approach—Over a 15 month period, 11 patients were implanted with platinum micro-wire bundles into mesial temporal structures. Protocols were developed for A) monitoring electrode integrity through impedance testing, B) ensuring continuous 24-7 recording, C) localizing micro-wire position and “splay” pattern and D) monitoring grounding and referencing to maintain the quality of recordings.

Main Result—Five common modes of failure were identified: 1) broken micro-wires from acute tensile force, 2) broken micro-wires from cyclic fatigue at stress points, 3) poor *in-vivo* micro-electrode separation, 4) motion artifact and 5) deteriorating ground connection and subsequent drop in common mode noise rejection. Single neurons have been observed up to 14 days post implantation and on 40% of micro-wires.

Significance—Long-term success requires detailed review of each implant by both the clinical and research teams to identify failure modes, and appropriate refinement of techniques while moving forward. This approach leads to reliable unit recordings without prolonging operative times, which will help increase the availability and clinical viability of human single neuron data.

[6]Please address correspondence to Karen A Moxon Km57@drexel.edu.
[*]Indicates equal contribution

Disclosure
The authors report no conflict of interest concerning the materials or methods used in this study or the findings specified in this paper.

Keywords

Single Unit Recording; Epilepsy; Micro-wires; Depth electrodes; Human

1. Introduction

Single neurons recordings from human subjects is becoming of increasing interest to neuroscientists and engineers alike as our understanding of the role of single neuron activity in cognition, motor control, and information processing becomes better understood. It is now well established that patterns of single neuron activity convey information about the state of neuronal networks, sensory input, and motor output. (1) (2, 3) Therefore, changes in these patterns of activity after neurological injury or disease, can provide insight into the underlying mechanisms of the disorder and potentially, insight into therapeutic interventions. While numerous studies have employed either multielectrode arrays (cortical recordings)(4) or micro-wire bundles (mesial structure recordings) (5–8) to record single neuron activity in humans, few provide specific methodological details about the required troubleshooting approaches for successful recordings, especially from mesial structures. As a result adoption of single neuron recording protocols has been restricted to a few clinical sites worldwide (9–15), and consequently the pool of single neuron data available to researchers has been limited. In an effort to improve recordings and lower perceived barriers to implementing single neuron recording protocols, using micro-wire bundles, we studied failure modes and developed protocols to reduce the failure rate and improve the probability of high yield single neuron recordings from mesial temporal structures in humans.

The most common method to obtain *in vivo* neuronal activity is through extra-cellular recordings, in which a small micro-wire (<60 μm) is manually placed in the immediate vicinity of an intact neuron (16). Using single tungsten electrodes, micro-wire arrays, and drivable tetrodes, extracellular neuronal recordings have long been a staple of animal electrophysiology studies. Indeed, if these electrodes are placed close enough to a neuron, activity from a single cell can be obtained (single-unit activity; SUA). Failing this, it remains possible to record multi-unit activity (MUA) from the collection of cells in a somewhat larger neighborhood around the recording site (17, 18). In animal studies, both SUA and MUA have been used to gain a mechanistic understanding of the neural origin of cognitive function as well as pathophysiology.

For a variety of technical reasons, extracellular SUA/MUA recordings are more difficult to obtain in humans. These technical considerations understandably dissuade clinicians from recording neuronal activity in the modern clinical setting, which places a premium on minimizing operative time and streamlining surgical protocol. Compounding this problem, SUA/MUA recordings do not have a well-defined role for clinical application in intracranial monitoring for epileptic foci localization (19). Neuronal recordings are thus obtained almost exclusively for basic science research purposes, unrelated to the clinical problem of seizure localization. Indeed, there is limited opportunity to apply SUA/MUA recordings toward clinical and diagnostic use.

There is a growing gap between data that are clinically relevant and data that reflect the underlying pathophysiology of neurological diseases, such as epilepsy. The former is focused on the macroscopic level and the latter is caused by abnormal firing patterns of individual neurons. To bridge this gap, it is necessary to increase the availability of human single neuron data. With this goal in mind, we document the technical challenges that impede established methods for extracellular SUA/MUA recordings (20) in the clinical setting, with the intention of broadly disseminating methods to overcome these challenges. We have found that these methods can be implemented to reliably and efficiently record SUA/MUA in humans, as described in this report.

2. Materials and Methods

2.1 Patients

The presented methods for chronic SUA/MUA recording were developed in 11 patients who underwent implantation of intracranial depth electrode patients at Thomas Jefferson University's Epilepsy Monitoring Unit. This represented the entire population of consenting patients requiring (intracranial) electroencephalography (EEG) with depth electrodes during the study period. All research protocols were approved by the Thomas Jefferson University Institutional Review Board *(Philadelphia, PA)* and adhere to guidelines governing human subjects research as put forth by the Office for Human Research Protections of the US Department of Health and Human Services (45 CFR 46.100:505) of the Thomas Jefferson University Office of Human Research. All study candidates gave informed consent to participate in implantation of additional micro-wire and data collection.

2.2 Electrodes

Extracellular neuronal recordings were obtained from commercially available FDA approved combined macro-micro depth electrodes (Behnke-Fried depth electrode and inner-wire bundle; Ad-Tech Medical, Racine WI), based on the design initially developed at UCLA (20, 21). The electrode is manufactured as two separate components (Figure 1). The clinical component (henceforth referred to as the Behnke-Fried Depth; BFD), consists of 8 standard cylindrical, depth macro-electrodes (90–10 platinum iridium contacts, 1.3 mm in diameter, 0.8 mm in length) that are embedded on the surface of a silastic tube with a hollow lumen. The research component (henceforth referred to as the inner-wire bundle; IWB), runs through the lumen of the BFD and consists of 8 micro-wires (90–10 Platinum-Iridium; 40 micron diameter; Teflon insulation) and 1 reference wire (an additional micro-wire stripped of insulation). A protective sheath slides along the IWB to facilitate threading into the lumen of the corresponding clinical BFD (see Figure 1). The wires terminate in a pigtail-type configuration that connects to a 10 contact Cabrio® connector (AdTech Medical, Racine, WI). To create a connection between the unsterilized ohmmeter and the sterile surgical field, we mated the micro-electrodes with a sterilized Cabrio connector and a sterilized 5-ft customized extension ribbon cable. The extension cable was then mated to a non-sterilized custom breakout box, which was built to allow access to individual micro-wires and the un-insulated reference.

2.3 Implantation procedure

With experience gathered over 11 patients, we have developed a protocol to implant the BFD-IWB electrode. This protocol has been used to record neuronal activity reliably in each patient and consists of the following steps. First, we assemble the equipment needed to cut and implant the electrodes: the IWB and BFD pieces, a 15-blade scalpel, an open container of saline, a clean cutting surface, a sterilized Cabrio connector with a custom 5-ft extension cable, the ohmmeter with custom tip-jack breakout box, and a custom 1.5-mm inner diameter Large Bore Passing Needle (LBPN; AdTech Medical, Racine, WI). Next, we thread the IWB through the BFD and manually manipulate the microelectrodes until they hold a splayed pattern. (Figure 2C) This should be differentiated from the as-received state of the micro-wire bundle depicted in Figure 1A. With the IWB threaded through the BFD, we then check the impedances of the micro-wires (see section *2.3: Impedance Testing*), cut the micro-wires, and re-check the impedances. Each micro-wire is cut individually, at different lengths (ranging from 1–5 mm) with a fresh 15-blade. Obtaining both pre- and post-cut impedances ensures that the surface of each micro-wire is properly exposed. Threading the IWB through the BFD before the micro-wires are cut (1) establishes that IWB-BFD is free of manufacturing errors that would otherwise prevent a successful implant and (2) allows us to visualize the final, desired splay pattern of the micro-electrodes before implantation. The IWB is then removed from the BFD and set aside until implantation.

In the following text, we outline our implantation method, which is illustrated with an example case of a left sided craniotomy for the placement of depth and subdural strip electrodes (see Figures 2–4). All implantations were performed by, or under the direct supervision of, the same neurosurgeon. Before incision, we used scalp fiducial markers to co-register the three-dimensional surgical field to pre-operative magnetic resonance imaging (MRI), to allow for precise positioning of the BFD in the targeted structures using an image guided, frameless stereotactic approach. For all patients the targeted structures were hippocampus or amygdala. After exposure of the implantation site, the pia arachnoid is cut to allow entry of the BFD through the cortex. (Figure 2A). At this time, a flexible arm with adjustable rigidity was fixated to the headframe and the LBPN was tunneled 3–5 cm through subcutaneous tissue from the incision boundary to a convenient exit site (Figure 2B). Next, the image guidance tool (Stryker, Kalamazoo, MI) is attached to the flexible arm in order to locate the target structure on the pre-op MRI; once the target was accepted, the arm was locked into place (Figure 2D). Then, using the slotted electrode guide, the BFD was implanted to the appropriate depth in order to reach the target structure (Figure 2E). All BFD's were placed using a transverse temporal approach. With the BFD in place, the IWB was threaded through the lumen of the implanted BFD. The IWB was slowly advanced by hand to engage the tissue beyond the distal tip of the BFD, and the IWB was coupled to the BFD at the proximal end (Figure 2F). The coupled BFD-IWB complex was then passed subcutaneously through the LBPN to the exit site (Figure 2G). Finally, the BFD-IWB was affixed to the skull via a rigid surgical fixation plate adjacent to the edge of burr hole/craniotomy (not shown). The number of implanted depth electrodes was determined by the number of mesial sites required for each patient's diagnostic study. Once all electrodes were implanted and tunneled (Figure 2H), the exposure was closed in routine manner.

2.4 Post-implant monitoring

After implantation, the electrodes (BFD-IWB) were carefully wrapped in a bandage to create a “headwrap”. The micro-wires were made accessible within the headwrap to measure post-op impedances. Patients recovered in the intensive care unit overnight. After recovery, patients were moved to the epilepsy monitoring unit (EMU). Clinical electrodes were connected to an EEG monitoring system (Nihon Kohden, Tokyo, Japan) using standardized cable interconnects (Integra, Plainsboro, NJ). Under the supervision of the research team, technicians then connected the micro-wires of the IWB to custom Cabrio adapters and a headstage pre-amplifier (HS-36h, Neuralynx, Bozeman MT). The headstage preamplifier and all excess wire were securely wrapped to the patient's skull for the duration of the patient’s stay. Amplified micro-wire signals were sent to a high-speed data acquisition system (Digitalynx S, Neuralynx, Bozeman MT) using shielded 25-ft tethers, which were less restrictive than the analogous clinical tethers. Recordings began immediately after the initial hook-up. Signal quality optimization will be discussed in the results section.

2.5 Impedance testing

We isolated micro-electrode breaks by performing routine impedance testing. Using a clinically approved impedance meter (model IMP-1; Bak Electronics, Sanford, FL), electrode impedance was measured at the following time points: 1) post sterilization (ex-vivo), 2) post final-cut (ex-vivo), 3) post implantation, 4) postoperatively, 5) when the patient arrived on the neurological intensive care unit (NICU), 6) when the patient arrived on the long-term epilepsy monitoring unit (EMU), and 7) periodically over the course of the recording.

All impedances measurements were made between individual micro-wires and the internal reference wire whenever possible. In cases where the reference wire was broken, an intact micro-wire was used in its stead. Ex-vivo impedances were performed in sterile saline. Typical impedances of intact electrodes ranged between 50 and 500 kΩ. Measurements greater than 1MOhm were considered open. Post-implant measurements were consistently 20–30 kΩ higher in-vivo versus the saline bath. An example of impedance measurements for the entirety of an example patient’s hospital stay is given in Figure 3B. We note that Figure 3B displays a different patient than Figures 2, 4, and 5. This is done to show an example of how micro-electrode impedance changed as a function of time, which we only recorded in the first 4 patients. After the first 4 patients, we began wrapping the electrodes in the patients headwrap. This helped stabilize the electrodes (see section 3.2.4), but complicated access to the micro-wires for daily impedance measurements.

2.6 Bench testing

In the results, we document the various “failure modes” of the micro-electrodes. A failure mode is defined as a discrete set of circumstances leading to an irreparable decrease in the signal-to-noise ratio (SNR) of the micro-wire recording. To more precisely characterize these failure modes, we performed a series of bench tests to reproduce failure in a controlled laboratory setting. The data collected during these bench tests allowed us to formulate more accurate hypotheses regarding the cause of the failure modes and more effectively design workarounds.

Some electrodes experienced a sudden and severe drop in SNR, which we attributed to discrete micro-electrode breaks. To simulate this failure mode, we quantified the absolute tensile strength required to break the IWB. This value served as a loading threshold; forces beyond this threshold would necessarily break the micro-wires. A benchtop simulation was run on 3 sample IWBs (identical to those used during implantations). It is important to note that the IWB was tested without the BFD to simplify the testing apparatus. It was determined that the silastic material of the BFD is easily deformed and any tensile loading would quickly shift stress to the more rigid platinum wires of the IWB. Axial tensile loading was performed with a Bose Electroforce 3200. Samples were prepared by removing the protective sheath and clamping the IWB into two knurled clamps spaced 10 cm apart. The clamping causes all micro-wires to short to the reference microelectrode. Micro-wires were submerged in sterile saline. Starting at 0N, axial tension was increased in increments of 0.5N. After each increment, impedance measurements were made on the reference micro-wire. As during surgery, typical reference electrode impedances were between 5 and 10 kOhm. Failure was identified by an increase in impedance and a corresponding jump in the generated stress-strain curve.

Other microelectrodes exhibited a gradual and steady degradation of SNR over time, which we attributed to cyclic tensile loading at sub-threshold loading values. To simulate this, a bench-top apparatus was developed to mimic the inner wire bundle configuration during implantation. A single metal plate lined with a 2mm foam rubber pad created a flexion point to act as a stress concentrator. The wire bundle was then deflected to 80 degrees from the horizontal and a 3N impulse was applied every 2 seconds for 50,000 loading cycles. Impedances were recorded periodically to see if cyclic sub-threshold loading at a stress concentrator could break micro-wires. Two IWBs were tested in this configuration and compared to in-vivo impedance measurements.

Unit yield was dependent on the degree of micro-wire splay in neural tissue (see Figure 4B). To actually visualize splay, a benchtop agar model was used. To mimic brain tissue, a clear agar gel was cast in a square plexiglass chamber. Using published values of Young's modulus and the Poisson ratio of brain tissue (22), a reduced modulus was calculated and compared to published agar concentration-reduced modulus curves(23). It was determined that a 0.4% agar solution approximates the elasticity of brain tissue. Once solidified, a polyimide tube with the same inner diameter as the lumen of the clinical depth electrodes was inserted into the gel. Two inner wire bundles, one mechanically deformed to encourage splay, and the other as delivered by the manufacturer, were prepared. Inner wire bundles were threaded into the polyimide tube and the protective sheath withdrawn. Inner wire bundles were advanced so that 5mm of micro-wire extended beyond the polyimide tube (this approximates the amount of micro-wire that engages tissue in-vivo). High resolution photos were taken to document splay and the electrode was withdrawn. The process was repeated 5 times for each electrode.

2.7 Unit identification & analysis

SUA/MUA was manually confirmed using Offline Sorter (Plexon, Dalas TX) following established techniques (24). In brief, raw data was high pass filtered at 396 Hz, and a

threshold was set at 4.5 standard deviations about the mean amplitude. 4 msec waveforms were captured about each threshold crossing and candidate waveforms were plotted in 3 dimensional principal component space. SUA/MUA was identified by a spatial clustering in principal component space. A noise cluster was identified and excluded from further analysis. SUA was identified when isolated clusters contained fewer than 0.5% of spikes within 1 msec of one another and an autocorrelogram that showed evidence of the refractory period. MUA was identified as isolated clusters where between 0.5% and 3% of spikes occurred within 1 msec of one another.

When comparing yields, it is important to note that many published human single neuron studies record activity over the course of several sessions spread out over the course of the patient's stay. With these discrete recording events, it is not possible to definitively track neurons seen on one day to the next. As a result neurons recorded during different recording sessions are treated independently. To avoid bias, we took random 2.5 hour recordings from each day of the patient's stay and have reported the recording with the largest number of identified single units and report yield from this recording alone

3. Results

3.1 Single- and multi-unit neuronal recordings

Using the protocol described in the methods section, we recorded extracellular SUA/MUA from 11 patients implanted between November 2011 and February 2013. Over thirty-two random 2.5 hour recording sessions within these 11 patients, 125 single units and 39 multi-units were successfully identified An example of unit activity recorded from the patient presented in Figures 2 and 4 is provided in Figure 5. For the 11 patients presented, four had two depth electrodes, three had three depth electrodes and four had four depth electrodes. Single neurons were recorded as far as 2 weeks post implantation but on average recordings persisted for 7 +/− 3 days with over 50% of recordings limited by the clinical decision to proceed with resection. On average, each BFD-IWB (8 micro-wires) recorded a maximum of 2.1+/−0.9 single neurons. Before failure modes were identified and workaround protocols were developed, the average single neuron yield per depth electrode was 1.4+/− 0.5 (n = 3) single neurons per depth. After recordings were optimized to avoid the identified failure modes, the yield nearly doubled to 2.7+/−0.8 (n=3) single neurons per depth electrode. All patients had at least one multi/single unit during the last recording prior to deplantation.

3.2 Failure modes: overview

The primary goal of this technical report is to document the technical challenges encountered during the implantation and recording of extracellular neuronal signals, and also methods to overcome these challenges. In particular, whereas the methods used to record extracellular neuronal data using micro-wires are, in principle, similar to those used to record routine intracranial EEG, certain failure modes warrant description to mitigate their deleterious effects and allow reliable recordings of firing rate data. For some of these failure modes, we were able to change our protocol and improve recordings, resulting in high-amplitude units for the entire duration of a patient's hospital stay (~2 weeks). In the following sections, each observed failure mode is described and fully characterized,

including the hypothesized mechanism underlying the failure mode, any bench tests used to confirm the proposed mechanisms, the adopted workarounds, and the data to support their efficacy.

3.2.1 Failure Mode #1: Sudden loss of single neuron activity—The most common failure mode was that micro-electrodes periodically exhibited a sudden and complete loss of single neuron activity. By frequently measuring impedances throughout the patient's hospital stay, we were able to determine that this failure mode most often occurred during periods when the electrodes were physically manipulated (e.g.: surgical tunneling procedure, initial hook-up, headwrap changes, unhooking for imaging, etc). Discrete breaks in micro-electrodes were detected as sudden jumps in impedance (see Figure 3B).

We hypothesized that this failure mode was caused by breaks induced by excessive tensile loads placed on the micro-wires, as in the case of overly aggressive digital manipulation. Indeed, the 40 micron platinum wires that comprise the IWB are inherently fragile. The alloy used has an ultimate tensile strength (UTS) of between 400 and 700 MPa, meaning that each un-insulated micro-wire breaks at a tension load of ~0.90 N. However, the number of electrodes in the wire bundle and the Teflon insulation imparts some added tensile strength, making it necessary to empirically derive the UTS of the micro-electrodes. To do that, we conducted bench tests (see methods) that demonstrated broken wires at an applied force of 13+/−0.5N. To put this in perspective, the reported maximum flexion force of an adult human finger is ~120N (25). While the silastic tube of the BFD augments the yield stress of the fully assembled electrode, it's greater elasticity quickly transfers the majority of applied axial tension to the more rigid IWB. It is therefore no wonder that rigorous or inattentive digital manipulation of the micro-electrodes was a common failure mode.

Three methods were implemented to overcome this failure mode. First, a custom tunneling needle (LBPN: see methods) was designed to reduce electrode manipulation during tunneling, which we isolated as a step that was very prone to electrode breaks. The LBPN worked by minimizing strain on the electrodes as they passed subcutaneously. Second, we used customized electrodes that were 2 inches longer than the standard design (current length: 570 mm). The elongated electrodes allowed technicians excess slack when connecting electrode tails to the recording system, which minimized tensile force when hooking/unhooking the electrodes in the EMU. Third, and most importantly, the clinicians (M.R.S., A.D.S, and J.J.E) made sure that the entire clinical and research team understood the importance of minimizing excessive tensile force when physically manipulating the micro-electrodes for any reason.

It should also be noted that a new generation of BFD-IWB hybrid electrodes are available that addresses sudden micro-wire breakages due to tensile loading, specifically at the junction between the platinum micro-wire and the clinical connection site. The design tested in this study has a structural weak point (lower UTS) where platinum wires are soldered to their clinical contact pads (the component that is clamped onto by the custom Cabrio connector). The new design structurally reinforces this junction with epoxy, thereby reducing the likelihood of failure.

3.2.2 Failure Mode #2: Gradual loss of single neuron activity—A second common failure mode was a gradual decrease in SNR from micro-electrodes over time, leading to total loss of signal (presumed electrode break) or a loss of all unit activity from the electrodes. We hypothesized that this progressive electrode failure reflected micro-wires that were broken through cyclic *sub-threshold* (<13 N; see section 3.2.1) loading at a point where the micro-wire was weakened by electrode geometry (stress concentrator).

To test this hypothesis, we designed a cyclic fatigue model (see methods) and used the model to simulate cyclical sub-threshold tensile loading (Figure 3C). Confirming our hypothesis, both bench tested and in-vivo impedances demonstrated similar patterns (compare Figures 3B and 3C). Impedances start between 50 and 500 kΩ and slowly drift upward by 10–100 kΩ followed by sudden jumps to the MΩ range indicating a break in the micro-wire. Over time, broken wire termini occasionally come back into contact with each other causing sudden and transient drops in impedance back to the 50–500 kΩ range. The similarity in patterns between benchtop and in-vivo measurements supports our sub-threshold cyclic fatigue failure explanation for progressive electrode failure within the headwrap.

To minimize the degree of progressive electrode failure, we attempted to remove points where cyclic fatigue failure could occur. A gentle curve (as opposed to a sharp bend) was formed as the electrode left the burr hole. The electrode was fixed *flush* specifically not within the burr hole) to the skull in this position using a small surgical plate while not pinching the electrode. Similarly after the electrode tail exited the skin, the headstage was manually oriented to reduce the need for sharp bends. A tight outer headwrap ensured that the headstage and electrode tail maintained their relative positions during the recording as any shifts within the headwrap would introduce sharp bends.

3.2.3 Failure Mode #3: Electrode position and micro-wire splay—As single neurons are only captured within 250 microns of a micro-wire(17), placement of micro-wires in low-density cellular areas will result in poor neuron yield. Indeed, some micro-wires did not record any units despite a technically successful implant (no failure modes observed). We hypothesized that such micro-wires were not located near enough to active cells. Without intra-operative recording techniques and/or micro-drive technology, such outcomes are, in our estimation, unavoidable.

A more remediable failure mode, however, was the lack of a good “splay pattern” of micro-wires in neural tissue. In this context, splay pattern refers to the position of the micro-wires within an IWB with respect to each other (see Figure 4B for an illustration). Ever since the BFD-IWB design was first formalized, the splay pattern of the micro-wires was recognized as an important determinant of unit yield. Indeed, Babb et al. noted that “*the less traumatic “spray” insertion results in successful unit recordings on* more *micro-electrodes and for longer periods than when the wires remain in a bundle*" (21). We also observed that fewer units were recorded when electrodes stayed clumped together “in a bundle”, in neural tissue (Figure 4C) versus when they splayed out relative to each other (Figure 4D). In Figures 4C-4D, we identified the splay pattern using high-resolution post-op CT’s (<0.9 mm thick slices). In these scans, when micro-wires successfully splayed into neural tissue they

appeared to terminate in a “puff-of-smoke” (Figure 4C), while an unsuccessful splay terminated in a narrow radiopaque bundle (Figure 4B). Out of 33 BFD implanted during this study, ~76% demonstrated successful splay upon review of post-operative CT. Recordings from depth electrodes demonstrating micro-wire splay showed significantly more neurons (2.0+/−1.6 neurons n=76) than those that did not (0.9+/−1.1 n =23) ($p = 0.014$)

In order to increase the percentage of micro-wires that engaged neural tissue with the appropriate splay pattern, prior to implantation and during the final cut, the neurosurgeon physically deformed each wire to the desired splayed configuration and re-sheathed the end to thread the IWB into the lumen of the BFD. The goal here was to impart some degree of memory to the wires that would encourage splay as the inner wire bundle was advanced into tissue. Each wire was cut independently. Prior to implementing this technique approximately 29% of implanted IWB would fail to splay. After implementation, only 17% of implanted IWB fail to splay.

Postoperative CT provides only limited insight into how individual micro-wires of the IWB behave as they engage the tissue. We therefore implemented bench testing using an agar brain analog to investigate whether pre-deforming the micro-electrodes increases the likelihood of achieving the desired splay pattern. Specifically, using an agar model for neural tissue (see methods), we performed a mock implant using two IWBs: one mechanically deformed to encourage splay (as was done in the surgical setting), and the other as delivered by the manufacturer (the naïve electrode). While there was some degree of electrode splay from the naive electrode (1.2+/−0.4mm; Figure 3F), the electrode that was pre-deformed showed a considerable increase in the width of splay (4.0+/−1.2mm; Figure 3E).

3.2.4 Failure Mode #4: Motion artifact—Motion artifact can be an ambiguous term. Physiologic motion artifact refers to myogenic potentials contaminating EEG data, however this type of motion artifact is more problematic for scalp EEG. For intracranial and single neuron recordings, electronic motion artifact is the major concern. When connecting intracranial electrodes to a recording system, multiple coupling connectors are required to complete the circuit. As the patient moves, these coupling connectors can shift causing slight changes in impedance which are reflected in the recording as low frequency oscillations or intermittent voltage transients. In addition, in the case of unshielded cables, as conductors move through external magnetic fields (often generated by hospital equipment), transient currents may be generated that can contaminate recordings.

In our present recordings, motion artifact contaminations were avoided through several approaches. First, only shielded cables were used between the electrode tail and the recording system. Second, all electrical coupling connections were secured to minimize motion of the micro-electrodes relative to the headstage. Connections between the electrode tail, the Cabrio connector, and the Neuralynx headstage were stabilized with parafilm, and then securely wrapped in the patient’s headwrap. All connections outside the headwrap were modified to include a latching mechanism and were attached to the patient’s junction box with velcro. Lastly enough cable was used that the patient was never restricted in his/her movement and no tension was put on the wire or the couplers. Extra care was taken to make

sure that connections would not break during seizures. However, for safety, a single breakpoint was set up at the headstage to prevent patients pulling out electrodes by tugging on their wire bundle.

3.2.5 Failure Mode #5: Power line noise & ground loops—Power line contamination typically refers to 50 or 60 Hz electromagnetic interference that originates from power lines or other external voltage sources (26). The generated electric field can induce capacitively coupled currents in unshielded conductors which manifests as a superimposed alternating voltage on recordings. In an in-patient diagnostic setting, both hospital equipment and personal electronic devices can act as electromagnetic radiators and the patient, electrodes, and connecting cables can act as antennas. In general the easiest solution is to remove the source of the electromagnetic interference. In cases where this is not possible, the recording can be protected by shielding the recording cables and equipment. Shielding creates a faraday cage around the recording wires and hardware and prevents external electromagnetic interference. Shielded cables contain a conductive layer surrounding signal carrying wires. This conductive layer is connected to ground at one end of the cable, creating the faraday cage. It should be noted that connecting the shield to ground on both ends of the cable can introduce ground loops (see below). For equipment that doesn't have shielding, a grounded conductive cloth or aluminum foil can be used to the same effect.

Ground loops refer to situations where the electrical grounds of supposedly isolated devices are not at the same potential. The potential difference between circuits can generate a current that contaminates both devices. In the case of human recordings, different electrical outlets in the patient room may have slightly different ground potentials. Thus, connecting a clinical recording system and a research recording system to different outlets with different grounds may create a ground loop. The easiest way to compensate for ground loops is to ensure that equipment ground is short circuited across all devices.

To address power line noise and ground loops, custom shielded tethers and couplers were designed in conjunction with the manufacturer (Neuralynx, Bozemann MT). Both the research recording system and the clinical recording system were plugged into the same outlet to share electrical ground. The research system patient ground and the clinical system patient ground were also short circuited using a touchproof jumper cable. When necessary, a conductive silver cloth was wrapped around the headstage and grounded, which extended the faraday cage up to the patients headwrap. Proper patient grounding not only ensures that no ground loops occur, but also significantly improves the signal to noise ratio.

Lastly, the patient ground refers to a non-current carrying ground wire that is often times connected to the skin above the mastoid process. The human body tends to act as an antenna picking up electromagnetic contamination across the frequency spectrum. By recording the potential seen by the body as a whole it can be subtracted out of neural recordings, resulting in improved signal to noise ratio (common mode rejection). In this case the noise common to both the patient ground and the clinical recording can be rejected leaving only neural signal. Manifestations of poor common mode rejection due to poor grounding include

increased power line contamination, and an increase in the noise floor, particularly above 1000 Hz.

3.3 Additional considerations

In addition to the failure modes, there were a number of additional considerations. These issues were not severe enough to induce a failure mode per se, but needed to be addressed before neuronal data could be recorded in the clinical setting.

3.3.1 Additional considerations #1: Referencing schemes—Most modern recording systems allow for some flexibility in choosing a reference electrode. One option is to choose the reference to be a low-impedance contact in the vicinity of the micro-wire. Examples of such references include, the dedicated (stripped) micro-wire reference provided on the IWB by the manufacturer, the most distal macro-electrode contact on the BFD, or a macro contact that is found to be the subdural space based on post-operative imaging. For our recordings, All of these contacts performed equally well as low impedance (<10 kΩ) reference lines. The advantage of using a low-impedance reference was that it was guaranteed to be quiet with respect to unit activity: any unit observed could be localized to the micro-wire and not the reference line. However, the disadvantage was that using low-impedance contacts caused the SNR to increase. The suspected mechanism of this increase in SNR was that the low-impedance reference acts as more of a high pass filter than its micro-wire counterpart, and as a result the output of the differential amplifier has a poorer signal to noise ratio at higher frequencies. To combat this problem, we often recorded unit activity using another micro-wire as a reference, which had a similar impedance profile as the recording electrode. Because the reference micro-wire is in brain tissue and not CSF, single neuron contamination of the reference wire can artificially inflate the number of neurons detected. It is imperative to review all offline analysis for time locked inverted action potentials to ensure that the reference wire is single neuron free. Single neuron contamination being avoided, the micro-wire that most improved the signal to noise ratio was routinely chosen as reference.

3.3.2 Additional considerations #2: Input impedance on recording amplifier—Perhaps the most limiting factor to unit recording in the clinical setting is the cost needed to purchase an amplifier with appropriate input impedance to record from micro-wires. A high input impedance on the recording amplifier is needed to avoid impedance mismatch between the electrode and the amplifier. Impedance mismatch refers to signal distortion as a result of connecting a high impedance circuit (IWB) to a low impedance circuit (the differential input of a standard clinical amplifier and analog-digital-converter). The difference in impedance can cause signal reflections, where certain frequency components of the signal are reflected back to the brain instead of transmitted to the recording system. Modern single neuron recording systems avoid this through the use of a voltage buffering headstage. These headstages are designed to have an internal impedance (1–10GΩ) that is several orders of magnitude higher than the source impedance (100k-1MΩ). Standard clinical recording systems are meant to record from scalp or intracranial electrodes (1–10Ω) and have correspondingly lower internal impedances. Thus high impedance micro-wires recorded on standard EEG systems will likely produce distorted signals (27).

3.3.3 Additional considerations #3: alternative electrodes—Lastly, this study has focused exclusively on the use of the Behnke-Fried type of combined macro-micro electrode for single/multi-unit recordings from mesial temporal structures. It should be noted, however, that alternative devices are commercially available and FDA approved for recording in human patients. Hybrid depth electrodes (28, 29) have been designed where micro platinum contacts are interspersed along the shaft of traditional depth electrode in between existing macro contacts. Such devices share many of the same potential failure modes that have been discussed with the obvious exception of electrode splay. It is often the case that macro electrode contacts on traditional depth electrodes end up in white matter tracts. In the case of micro electrode contacts, such positioning fails to yield any usable single or multiunit activity, thus these devices require advanced design planning prior to implantation to ensure that microelectrodes are targeted to grey matter regions and not white matter tracts.

4. Discussion

4.1 Systematic review is critical to chronic recording—Out of all of the optimizations and techniques that have been detailed thus far, the single most important to the success of a chronic recording protocol is a detailed and systematic review of each patient prior to the next. Failures can be classified and potential failure modes can be assessed and confirmed with methodical testing. Once a failure mode is identified, potential solutions can be implemented and revised. Daily tracking of impedance measurements and review of the recorded data will help to isolate when recordings fail in an effort to find a corresponding event or noise source that might explain the failure. Review of video and nursing staff notes will help to track down outlier events that might corrupt the data, and dissection of deplanted electrodes can provide further insight into what elements of the recording setup are causing problems. Each component should be tested individually if possible, especially connectors and cables which are prone to mechanical failure, and signal generators and oscilloscopes should be used to test all other electrical equipment when electrodes are not available.

4.2 Necessary infrastructure—A majority of clinical sites that support in-patient diagnostic monitoring already have most of the infrastructure in place to support chronic single neuron recordings. Recording systems and electrodes are commercially available and FDA approved; surgical techniques are not prohibitively difficult; and single neuron recordings work in parallel to existing clinical recordings and do not preclude the ability to collect data to make clinical decisions for epilepsy. Other than minor financial concerns, the only remaining barrier is a matter of implementation. A dedicated research staff member must monitor and troubleshoot recordings and communicate findings with surgical and nursing staff. Nursing staff and technicians must be instructed on the proper handling of new equipment, especially the headstage preamplifier (as it has no counterpart in standard intracranial recordings) and the micro-wire electrodes (as they are more fragile and break under considerably lower tensile load than traditional clinical electrodes.) Lastly, several ancillary issues may need to be addressed. Synchronizing clinical and single neuron recordings (usually by means of jittered sync pulse) creates a richer dataset for analysis. Data storage must be arranged in advance, as a single patient with only 32 micro-wires may

generate as much as a terabyte of information over the course of their stay. Managing and analyzing that volume of data is challenge in itself. Automatic clustering algorithms like KlustaKwik (http://klustakwik.sourceforge.net) and Wave_clus (30) can identify potential single neuron activity, but should always be verified manually. Motion artifact, noise contamination and even the presence of action potentials on the reference can ruin a dataset and so recordings must be continuously screened for such.

4.3 Clinical relevance—Lastly, while we have stressed the importance of single neuron data sets in research settings, the clinical significance of single neuron recordings is not to be overlooked. Characterizing the behavior of neuronal subpopulations may allow insight into personalized treatment; and computational power and availability are quickly making this type of characterization achievable in therapeutically relevant timescales. In the coming decades, the diagnostic power of single neuron recordings will continue to grow, and we can accelerate this growth by adopting chronic single neuron recordings as standard practice for all intracranial diagnostic patients.

5. Conclusion

In conclusion, while single neuron recordings in human subjects have been around for the past five decades, only recently has the technology become readily available to roll out chronic single neuron recordings as standard protocol. With more centers adopting such protocols, the hope is that pool of available neural data will grow and more researchers will incorporate single neuron analysis and further our understanding of neural function.

Acknowledgments

This work was supported by National Institutes of Health grant MH55687 (M.J.K) and a grant from the Coulter Foundation (K.A.M). We thank Dale H. Wyeth, Edmund Wyeth, and Ryan B. Williams for technical assistance at Thomas Jefferson Hospital and Frank M. Kepics for technical assistance at Drexel University. We are indebted to all patients who have selflessly volunteered their time to participate in our study.

References

1. Rieke, F.; Warland, D.; de Ruyter van Steveninck, R.; Bialek, W. Spikes: exploring the neural code. Cambridge, {MA}: MIT; 1997.
2. Hebb, DO. Organization of Behavior. New York: Wiley; 1949.
3. Buzsáki G. Neural syntax: cell assemblies, synapsembles, and readers. Neuron. 2010 Nov; 68(3): 362–385. [PubMed: 21040841]
4. Maynard E, Nordhausen C, Normann R. The Utah intracortical electrode array: a recording structure for potential brain-computer interfaces. Clin. Neurophysiol. [Internet]. 1997; 102:228–239. Available from: http://www.sciencedirect.com/science/article/pii/S0013469496951760.
5. Babb TL, Wilson CL, Isokawa-Akesson M. Firing patterns of human limbic neurons during stereoencephalography (SEEG) and clinical temporal lobe seizures. Electroencephalogr. Clin. Neurophysiol. [Internet]. 1987 Jun; 66(6):467–482. Available from: http://www.ncbi.nlm.nih.gov/pubmed/2438112.
6. Babb TL, Crandall PH. Epileptogenesis of human limbic neurons in psychomotor epileptics. Electroencephalogr. Clin. Neurophysiol. [Internet]. 1976 Mar; 40(3):225–243. Available from: http://www.ncbi.nlm.nih.gov/pubmed/57852.
7. Verzeano M, Crandall PH. Neuronal activity of the amygdala in patients with psychomotor epilepsy. Neuropsychologia. 1971; 9(3):331–344. [PubMed: 4948323]

8. Dichter M, Herman C, Selzer M. Extracellular unit analysis of the hippocampal penicillin focus. Electroencephalogr. Clin. Neurophysiol. [Internet]. 1973 Jun; 34(6):619–629. Available from: http://www.ncbi.nlm.nih.gov/pubmed/4122397.
9. Bragin A, Engel JJ, Wilson CL, Fried I, Buzsáki G. High-frequency oscillations in human brain. Hippocampus [Internet]. 1999 Jan; 9(2):137–142. Available from: http://www.ncbi.nlm.nih.gov/pubmed/12325068.
10. Kawasaki H, Kaufman O, Damasio H, Damasio aR, Granner M, Bakken H, et al. Single-neuron responses to emotional visual stimuli recorded in human ventral prefrontal cortex. Nat. Neurosci. [Internet]. 2001 Jan; 4(1):15–16. Available from: http://www.ncbi.nlm.nih.gov/pubmed/11135639.
11. Rutishauser U, Schuman EM, Mamelak AN. Online detection and sorting of extracellularly recorded action potentials in human medial temporal lobe recordings, in vivo. J. Neurosci. Methods [Internet]. 2006 Jun 30; 154(1–2):204–224. Available from: http://www.ncbi.nlm.nih.gov/pubmed/16488479.
12. Worrell, Ga; Gardner, AB.; Stead, SM.; Hu, S.; Goerss, S.; Cascino, GJ., et al. High-frequency oscillations in human temporal lobe: simultaneous microwire and clinical macroelectrode recordings. Brain [Internet]. 2008 Apr; 131(Pt 4):928–937. Available from: http://www.pubmedcentral.nih.gov/articlerender.fcgi?artid=2760070&tool=pmcentrez&rendertype=abstract.
13. Alarcón G, Martinez J, Kerai SV, Lacruz ME, Quiroga RQ, Selway RP, et al. In vivo neuronal firing patterns during human epileptiform discharges replicated by electrical stimulation. Clin. Neurophysiol. [Internet]. 2012 Sep; 123(9):1736–1744. Available from: http://www.pubmedcentral.nih.gov/articlerender.fcgi?artid=3432232&tool=pmcentrez&rendertype=abstract.
14. Hefft S, Brandt A, Zwick S, von Elverfeldt D, Mader I, Cordeiro J, et al. Safety of hybrid electrodes for single-neuron recordings in humans. Neurosurgery [Internet]. 2013 Jul; 73(1):78–85. discussion 85. Available from: http://www.ncbi.nlm.nih.gov/pubmed/23615097.
15. Kreuz T, Chicharro D, Houghton C, Andrzejak RG, Mormann F. Monitoring spike train synchrony. J. Neurophysiol. [Internet]. 2013 Mar; 109(5):1457–1472. Available from: http://www.ncbi.nlm.nih.gov/pubmed/23221419.
16. Moxon, Ka; Nicolelis, M a L. Multiple-site recording electrodes. Methods simultaneous neuronal ensemble Rec. 25th–45th ed.. Boca Raton, FL: CRC Press; 1999.
17. Buzsáki G. Large-scale recording of neuronal ensembles. Nat. Neurosci. [Internet]. 2004 May; 7(5):446–451. Available from: http://www.ncbi.nlm.nih.gov/pubmed/15114356.
18. Gold C, Henze DA, Koch C, Buzsaki G. On the Origin of the Extracellular Action Potential Waveform: A Modeling Study. J. Neurophysiol. Am Physiological Soc. 2006; 95(5):3113–3128.
19. Engel AK, Moll CKE, Fried I, Ojemann GA. Invasive recordings from the human brain--clinical insights and beyond. Nat. Rev. Neurosci. 2005; 6:35–47. [PubMed: 15611725]
20. Fried I, Wilson CL, Maidment NT, Engel JJ, Behnke E, Fields TA, et al. Cerebral microdialysis combined with single-neuron and electroencephalographic recording in neurosurgical patients. J. Neurosurg. 1999; 91:697–705. [PubMed: 10507396]
21. Babb TL, Carr E, Crandall PH. Analysis of extracellular firing patterns of deep temporal lobe structures in man. Electroencephalogr. Clin. Neurophysiol. 1973; 34(3):247–257. [PubMed: 4129612]
22. Soza G, Grosso R, Nimsky C, Hastreiter P, Fahlbusch R, Greiner G. Determination of the elasticity parameters of brain tissue with combined simulation and registration. Int. J. Med. Robot. Comput. Assist. Surg. 2005; 01(03):87.
23. Nayar VT, Weiland JD, Nelson CS, Hodge a M. Elastic and viscoelastic characterization of agar. J. Mech. Behav. Biomed. Mater. [Internet]. Elsevier Ltd. 2012 Mar.7:60–68. Available from: http://www.ncbi.nlm.nih.gov/pubmed/22340685.
24. Brown ENEN, Kass RE, Mitra PP. Multiple neural spike train data analysis: state-of-the-art and future challenges. Nat. Neurosci. [Internet]. 2004 May; 7(5):456–461. Available from: http://www.ncbi.nlm.nih.gov/pubmed/15114358.

25. Hazelton FT, Smidt GL, Flatt aE, Stephens RI. The influence of wrist position on the force produced by the finger flexors. J. Biomech. [Internet]. 1975 Sep; 8(5):301–306. Available from: http://www.ncbi.nlm.nih.gov/pubmed/1184601.

26. Rangan, CS.; Sarma, GR.; Mani, VSV. Instrumentation Amplifiers. Instrum. Devices Syst. 2nd ed. New Delhi: Tata McGraw-Hill; 1997. p. 233-261.

27. Stacey W, Kellis S, Greger B, Butson CR, Patel PR, Assar T, et al. Potential for unreliable interpretation of EEG recorded with microelectrodes. Epilepsia. 2013 doi: 10.11.

28. Howard, Ma; Volkov, IO.; Granner, Ma; Damasio, HM.; Ollendieck, MC.; Bakken, HE. A hybrid clinical- research depth electrode for acute and chronic in vivo microelectrode recording of human brain neurons. Technical note. J. Neurosurg. [Internet]. 1996 Jan; 84(1):129–132. Available from: http://www.ncbi.nlm.nih.gov/pubmed/8613821.

29. Howard, Ma; Volkov, IO.; Abbas, PJ.; Damasio, H.; Ollendieck, MC.; Granner, M a. A chronic microelectrode investigation of the tonotopic organization of human auditory cortex. Brain Res. [Internet]. 1996 Jun 17; 724(2):260–264. Available from: http://www.ncbi.nlm.nih.gov/pubmed/8828578.

30. Quiroga RQ, Nadasdy Z, Ben-Shaul Y. Unsupervised spike detection and sorting with wavelets and superparamagnetic clustering. Neural Comput. [Internet]. 2004 Aug; 16(8):1661–1687. Available from: http://www.ncbi.nlm.nih.gov/pubmed/15228749.

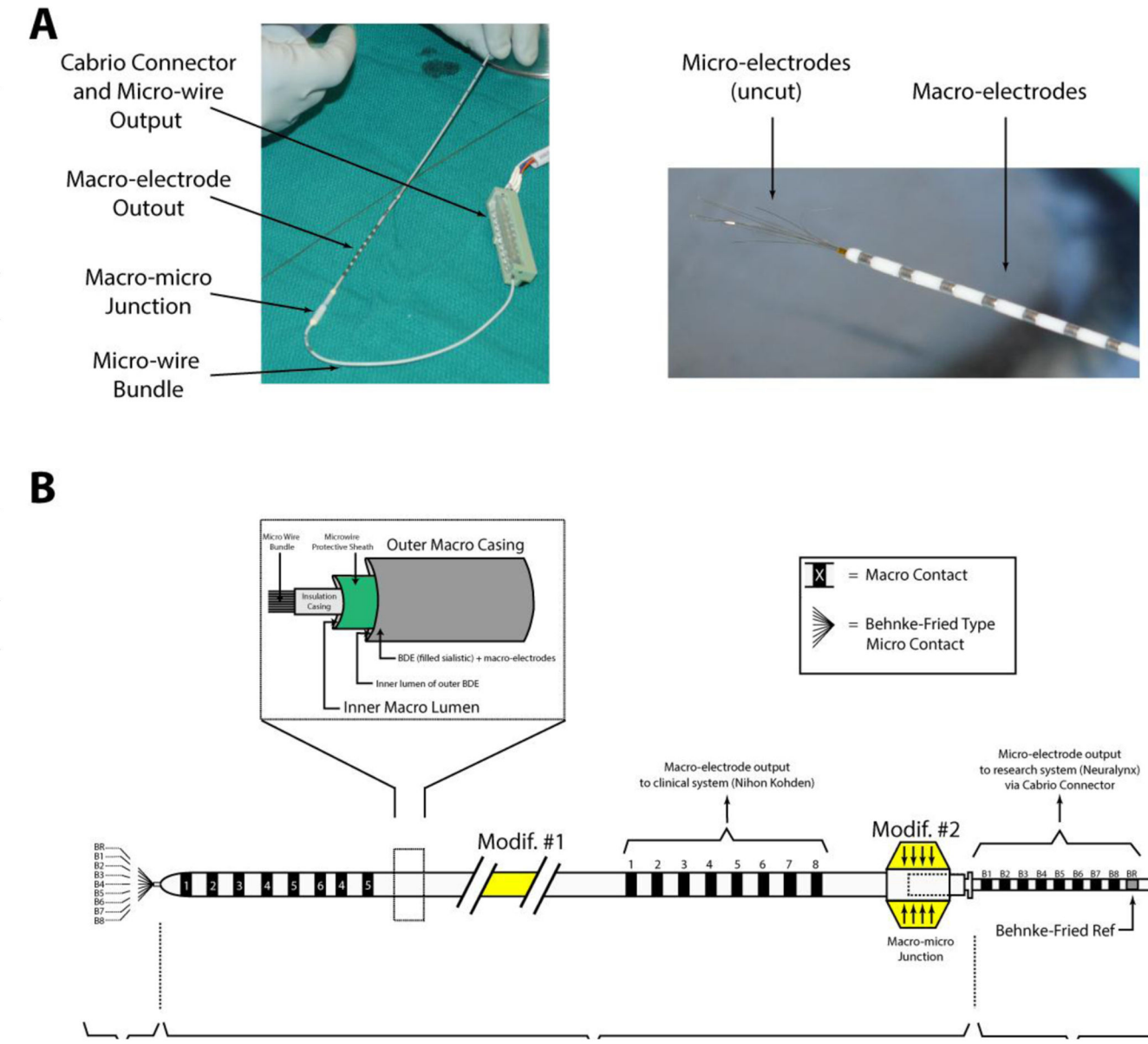

Figure 1. The electrode

A: The AdTech macro-micro electrode consists of an outer piece that houses the macro electrodes (BFD) and an inner piece that houses the microelectrodes (IWB). A Cabrio connector is used connect the output of the micro-wires to a downstream device (either ohmmeter or recording system). The macro- and micro-meet at their respective junctions. Right panel shows the projections of the micro-wires out of the end of the macro-electrode as received by the manufacturer. **B:** Schematic of the macro-micro electrode. Two modifications were implemented in our methods. First, (Modif #1), the electrode was lengthened by 2 inches to provide extra slack and minimize digital manipulation. Second, (Modif #2) The junction was minimized in width to fit through the large bore passing needle.

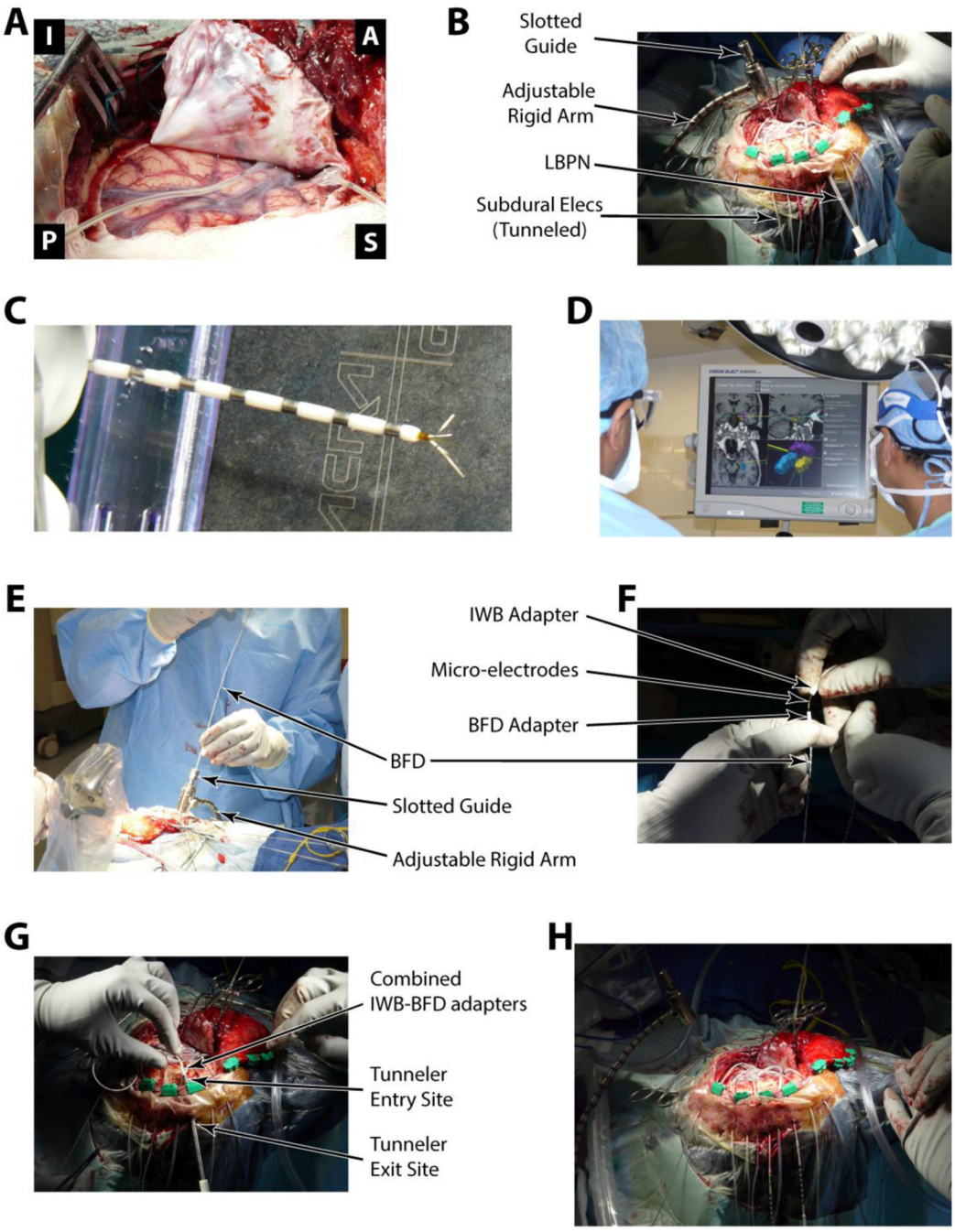

Figure 2. Illustration of implantation procedure

See methods (section 2.3) for a full description of each panel in the Figure in relation to electrode implantation.

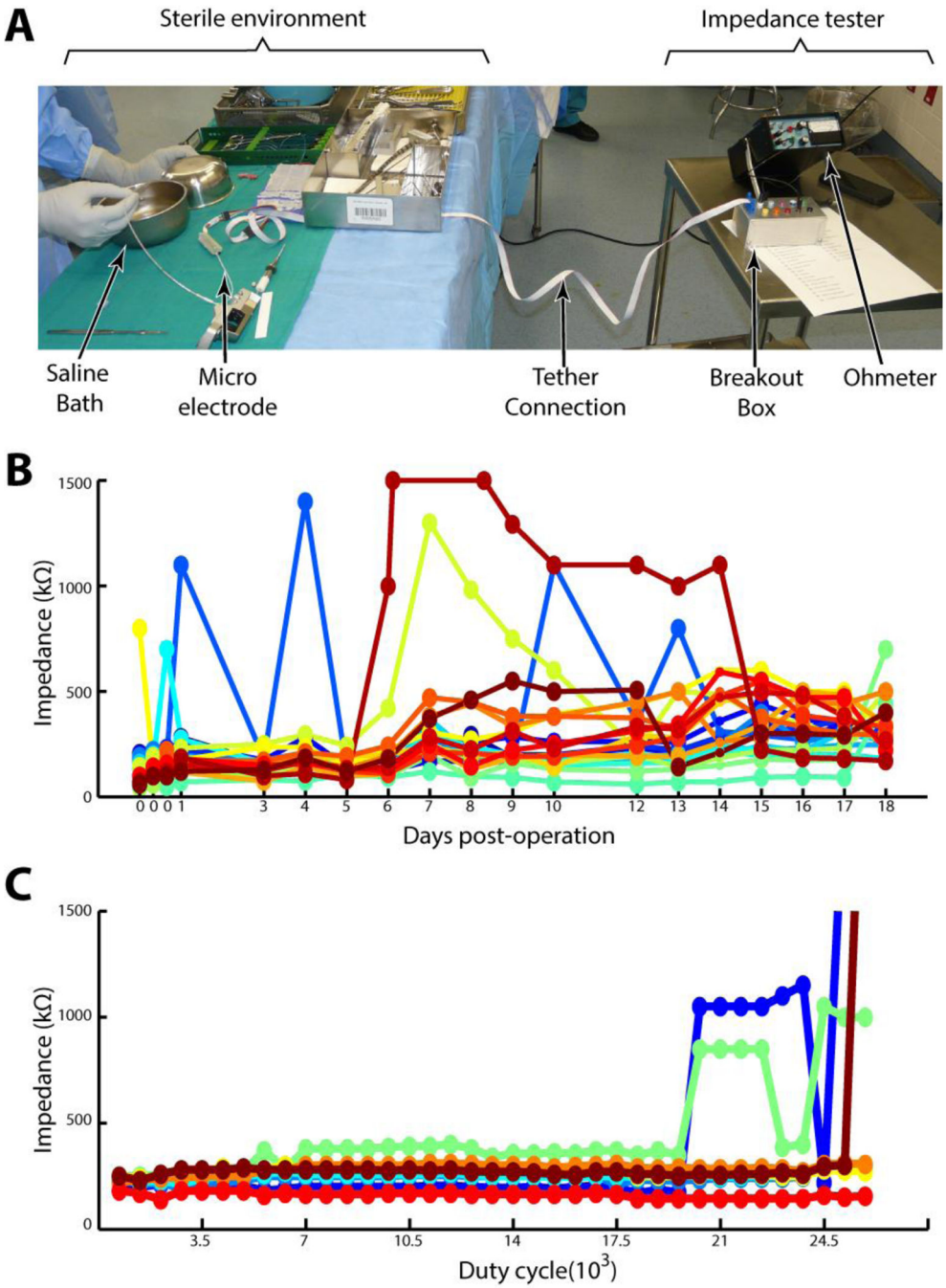

Figure 3. Impedance measurement

A: The set-up to measure impedances in the surgical environment. The left half of the figure represents the sterile field, the right half the non-sterile area where impedances were obtained by the research assistant. **B:** Impedances taken every day during one patient's hospital course. Each color represents a different micro-electrode. **C:** Impedances taken for 8 micro-electrodes using the fatigue bench-top simulation.

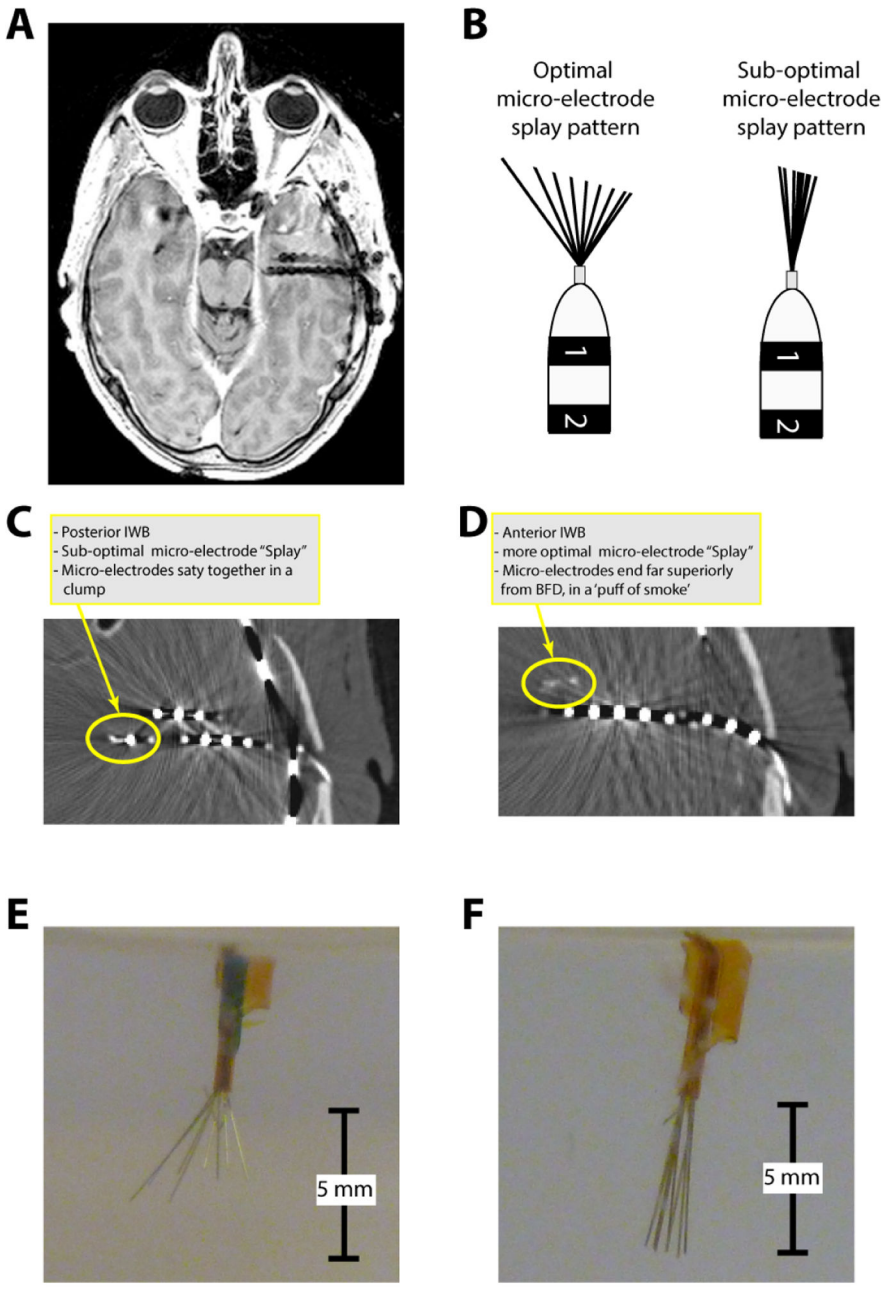

Figure 4

Figure 4.

Micro-electrode splay *in-vivo* and *ex-vivo*. **A:** Post-operative axial MRI of depth electrodes shown in Figure 2. **B:** Cartoon example of optimal and sub-optimal micro-electrode splay patterns and staggered micro-wire lengths. **C, D:** Thin sliced post-operative CT's of the posterior (C) and the anterior (D) depth electrodes. **E, F:** Benchtop tests of micro-wire splay patterns using pre-implantation induction of microelectrode splay (E) and simply implanting the naïve micro-electrode (F).

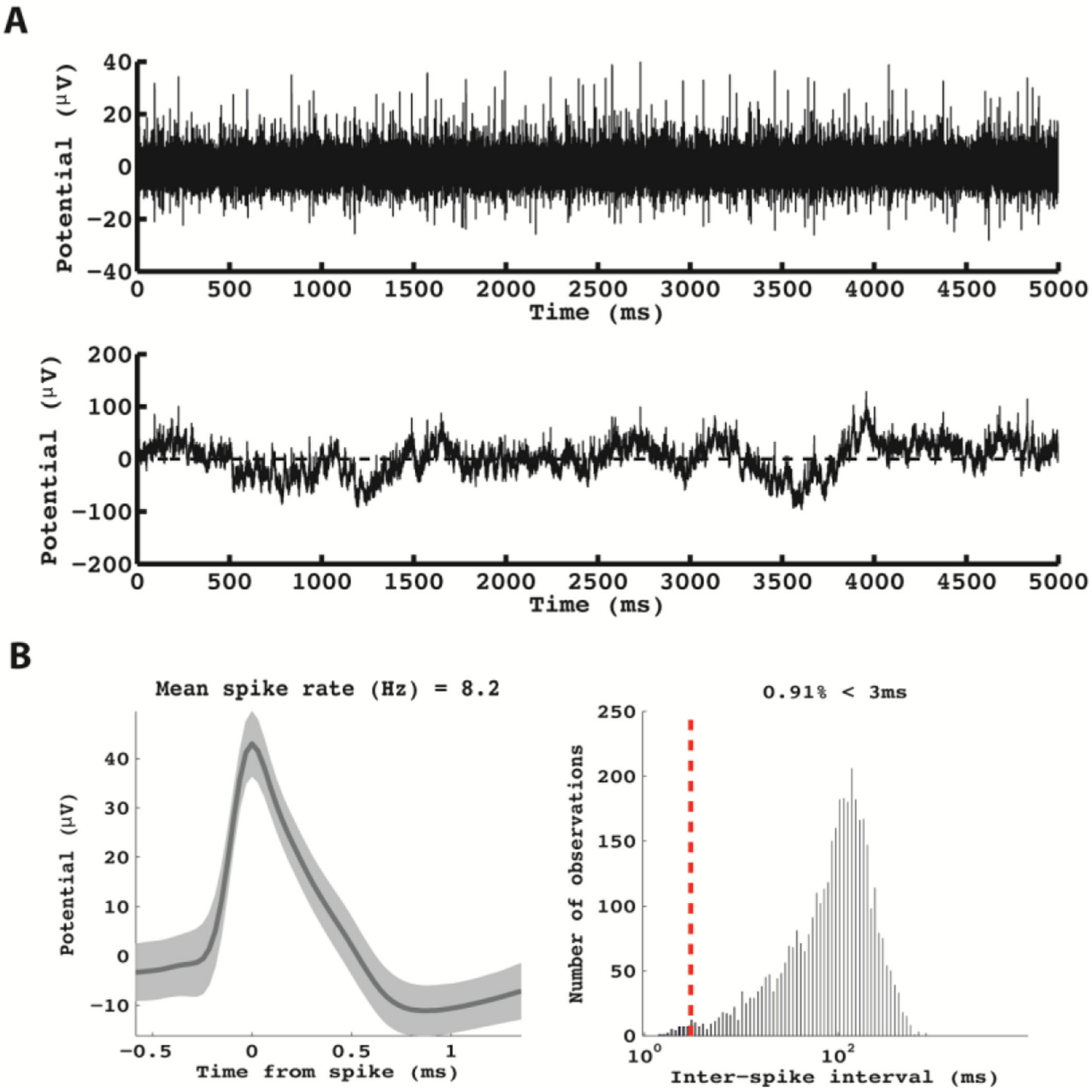

Figure 5.

Example of neuronal data obtained from the patient in Figures 2 and 4. This unit was recorded from the most anterior electrode. **A**: The raw (bottom panel) and pass-band filtered (300–9000 Hz, top-panel) raw voltage traces are shown for this micro-wire. **B**: The average waveform (left panel) and the distribution of inter-spike intervals (right panel) are shown.